Published in Applied Physics Letters 9, issue 142107, 1-3, 2007
which should be used for any reference to this work

Transition between grain boundary and intragrain scattering transport mechanisms in boron-doped zinc oxide thin films

J. Steinhauser,[a] S. Faÿ, N. Oliveira, E. Vallat-Sauvain, and C. Ballif
Institute of Microtechnology (IMT), University of Neuchâtel, Rue A.-L. Breguet 2, CH-2000 Neuchâtel, Switzerland

A comprehensive model for the electronic transport in polycrystalline ZnO:B thin films grown by low pressure chemical vapor deposition is presented. The optical mobilities and carrier concentration calculated from reflectance spectra using the Drude model were compared with the data obtained by Hall measurements. By analyzing the results for samples with large variation of grain size and doping level, the respective influences on the transport of potential barriers at grain boundaries and intragrain scattering could be separated unambiguously. A continuous transition from grain boundary scattering to intragrain scattering is observed for doping level increasing from 3×10^{19} to 2×10^{20} cm^{-3}

Transparent conductive oxides (TCOs) are an essential part of thin-film silicon solar cells. To contact the cell and act as a transparent window, TCOs have to exhibit a high conductivity and a high optical transmittance. In addition, they have to scatter the light at the TCO-cell interface in order to increase the effective absorption of light within the active layers.[1,2] Boron-doped zinc oxide (ZnO:B) layers deposited by low pressure chemical vapour deposition (LPCVD) have been intensively developed in our institute.[3] This material is especially attractive for thin-film solar cell technology, because of its low cost, and of the wide availability of its constituent raw materials. Furthermore, the LPCVD technique is well suited for large-scale device fabrication.[4] These films are constituted of large grains with a pronounced[9–18] preferential crystallographic direction. The extremities of the grains appear at the growing surface as large pyramids, which yield an as-grown rough surface texture that efficiently diffuses the light that enters into the solar cell.[1,3]

The optical and electrical properties of TCO films have been extensively investigated and recently reviewed. Ellmer[5] and Minami[6] discussed the limit of the resistivity of such films by analyzing reported data for ZnO films deposited by different techniques. They found that the electron mobility in undoped films is mainly limited by grain boundary scattering, whereas for doped layers intragrain scattering mechanism is predominant. But the transition between these two mechanisms within a given ZnO film series could not be evidenced yet. In the present work, the scattering mechanism limiting the electron mobility is determined by the comparison, of the value of the optical mobility (as evaluated by using the classical Drude model) with the value of the Hall mobility. When both values are markedly different, the mechanism limiting the electron mobility is attributed to grain boundary scattering. When both values are similar, the limiting mechanism is attributed to intragrain scattering. This approach is commonly applied to other TCOs.[7–11] The wide range of carrier density easily achievable in boron-doped LPCVD ZnO by varying the gas flow ratio allows us to observe within one single film system the transition from one transport mechanism to the other. The results of this contribution are consistent with previous analysis of the temperature dependence of the conductivity,[12] and constitute an experimental evidence of the transition between grain boundary scattering and intragrain scattering as the microscopic mechanisms limiting electron mobility in LPCVD ZnO. Consequently, further improvement of ZnO conductivity will have to be conducted depending on the type of transport mechanism dominant in the doping range of interest.

ZnO layers were deposited at low temperature (155 °C) by LPCVD on 0.7 mm thick Schott AF45 glass substrates. Diethyl zinc (DEZ) and water vapor were used as precursors and directly evaporated in the system. DEZ and H_2O flows were set to 13.5 and 16.5 SCCM (SCCM denotes cubic centimeter per minute at STP), respectively. Diborane (B_2H_6) diluted at 1% in argon was used as doping gas. The gas phase doping ratio $[(B_2H_6)/(DEZ)]$ used during ZnO deposition was varied from 0 (nominally undoped ZnO) to 2 (heavily doped ZnO). The optical transmittance (T) and reflectance (R) of ZnO layers on glass substrates were measured in air with a double beam Perkin-Elmer photospectrometer with integration sphere. A 1720X Perkin-Elmer Fourier transform infrared spectrometer was used to measure the normal reflectance spectra in the infrared region. The thickness of the layers was determined by a mechanical profiler. The resistivity ρ, the Hall carrier concentration N_{Hall}, and the Hall mobility μ_{Hall} were deduced from Hall measurement using a Van der Pauw configuration at room temperature. Various grain sizes were obtained at each doping level by varying the thickness of the films from 0.5 to 5 μm. The average projected area of the grain surface observed on scanning electron micrographs of the polycrystalline layers surface was measured using a commercial image analysis software (METRIC 8.02), and its square root value (δ) was taken as the dimensional parameter (thereafter to be called "grain size"). Note that, due to the growth mechanism, the grain size increases linearly over the film thickness.[3] This effect has no influence on the optical measurements, whereas the conductivity and Hall mobility are slightly reduced compared to the case where the grain size would be constant over the thickness.

Figure 1 shows the reflectance (R) and transmittance (T) spectra for 2.1 μm thick ZnO layers grown with various gas

[a]Electronic mail: jerome.steinhauser@unine.ch

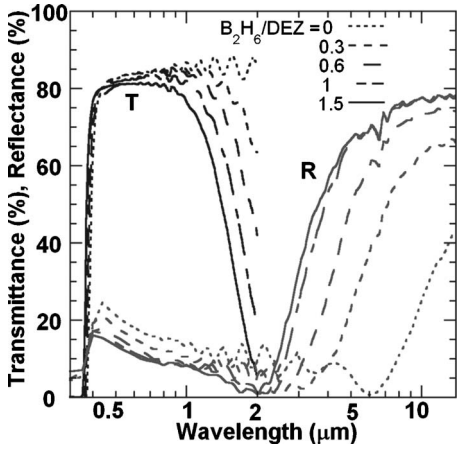

FIG. 1. Total transmittance (T) and reflectance (R) for 2 μm thick ZnO films, for which the gas phase doping ratios (B_2H_6/DEZ) used during the deposition was varied from 0 (undoped) to 1.5 (higly doped).

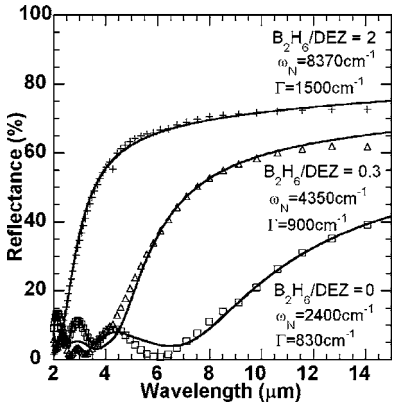

FIG. 2. Example of fits (solid lines) of near normal reflectance spectra of ZnO films (symbol) deposited with different gas phase doping ratios (B_2H_6/DEZ) using the Drude model.

phase doping ratios [(B_2H_6)/(DEZ)]. These films have an average transmittance superior to 80% and an absorbance close to zero in the visible range (0.4–0.8 μm). In the near infrared (NIR) region (wavelength between 0.8 and 2.5 μm), T decreases. The inflection point in the transmittance curves is shifted towards shorter wavelengths with increasing doping ratio due to the related increase of free carrier absorption (FCA). At longer wavelengths, R abruptly increases after the plasma resonance wavelength, which is progressively lowered as the boron content (and consequently the free carrier density) is increased. This behavior is generally described by the Drude model;[8–10] some authors use an extended Drude model including a Lorentz oscillator term[11] or a frequency dependent damping term.[13] Indeed, the Drude model in its simplest form is sufficient to describe the NIR optical behavior of LPCVD ZnO films. Consequently, the dielectric function ε can be expressed as

$$\varepsilon(\omega) = \varepsilon_\infty - (\omega_N^2/(\omega^2 + i\Gamma\omega)), \tag{1}$$

where ε_∞ is the high frequency dielectric constant, Γ is a damping frequency, and

$$\omega_N^2 = N_{\text{optic}} e^2/\varepsilon_0 m^*, \tag{2}$$

where N_{optic} is the free electron density, e the electron charge, ε_0 the permittivity of free space, and m^* the electron effective mass. The optical mobility μ_{optic} is calculated using the relation

$$\mu_{\text{optic}} = e/\Gamma m^*. \tag{3}$$

Assuming $\varepsilon_\infty = 4$ and $m^* = 0.28 m_e$ where m_e is the electron mass,[5,8] the reflectance spectra of ZnO films were fitted to this model taking into account the multiple reflection due to the air/glass/ZnO structure of our samples and using ω_N and Γ as fit variables. Examples of fits for ZnO layers with different doping ratios are given in Fig. 2. A good convergence of the fitted curves is obtained in the range of validity of the Drude model. The optical mobility μ_{optic} and carrier density N_{optic} are then extracted using Eqs. (2) and (3). The calculated electron mean-free path is in the range of a few nanometers and under the application of a rapidly oscillating electric field, the average electron path length is also much smaller than the typical grain size.[6,14] Therefore, grain boundary scattering will not influence the measured value for the optical mobility, and only intragrain scattering will influence μ_{optic}. Note that the depleted region at grain boundaries occupies only a small volume compared to the bulk of the grain and will not affect the optical measurements. In the case of the Hall effect measurement, electrons cross several grain boundaries, and consequently the grain boundary density will influence the measured value of μ_{Hall}.

For all measured samples, the value of the Hall electron density is the same as the one deduced from the optical measurements. As shown in Fig. 3, μ_{Hall} and μ_{optic} are both measured as a function of the grain sizes δ for ZnO series with two different carrier concentrations. For ZnO layers with low carrier concentration ($N = 3.8 \times 10^{19}$ cm^{-3}), the Hall mobility depends on δ: it increases from 22 to 36 cm^2 V^{-1} s^{-1} with increasing grain size. The optical mobility of these samples remains constant at a high value of 38 cm^2 V^{-1} s^{-1} for all grain sizes. For heavily doped samples ($N = 2 \times 10^{20}$ cm^{-3}) both Hall and optical mobilities remain nearly constant at a value around 25 cm^2 V^{-1} s^{-1} while δ is increased.

In lightly doped ZnO films, the observed differences between optical intragrain mobility and Hall mobility values are due to a grain barrier limited mobility, in agreement with previous observations described, for instance, by Seto[15] or Bruneaux *et al.*[16] As the grain size is increased, the grain boundaries influence on μ_{Hall} is reduced and μ_{Hall} and μ_{optic} become almost identical. For δ larger than 600 nm, the grain boundary density becomes too low to influence the measured Hall mobility. Consequently, efforts to improve the film conductivity by increasing the grain size beyond this value are useless. At heavy doping level, grain boundary scattering

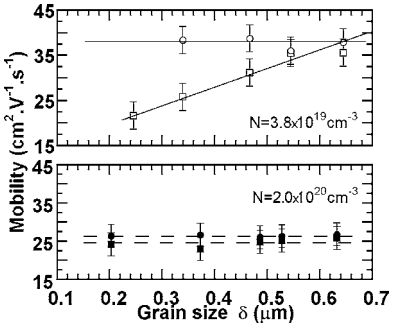

FIG. 3. Optical (circles) and Hall (squares) electron mobilities as a function of grain size for films with carrier densities $N = 3.8 \times 10^{19}$ cm^{-3} (open symbol) and $N = 2 \times 10^{20}$ cm^{-3} (filled symbol). The lines are guides for the eyes.

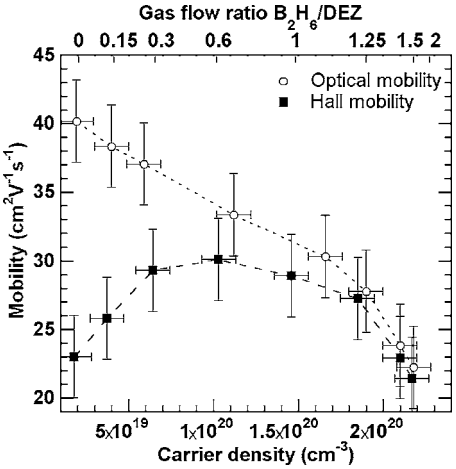

FIG. 4. Optical and Hall mobilities vs free carrier density for ZnO films grown with gas phase doping ratio (B_2H_6/DEZ) varied from 0 to 2. The lines are guides for the eyes.

plays only a minor role compared to intragrain scattering mechanisms. Here, the optical and Hall mobility values become almost identical and the variation of grain size does no longer affect the Hall mobility.

To find the doping level at which the main limiting scattering factor changes from grain boundary scattering to bulk scattering, films with a varying doping concentration at constant grain size have been fabricated. In Fig. 4, the optical and the Hall mobilities for samples with a variation of gas phase doping ratio $[(B_2H_6)/(DEZ)]$ from 0 to 2 are plotted versus the carrier density. The resistivity of these films decreases almost by a decade (from 1.4×10^{-2} to 1.2×10^{-3} Ω cm). This variation is mainly caused by an increase of free carrier density from 2.0×10^{19} to 2.2×10^{20} cm^{-3}. For lightly doped layers, μ_{optic} has a value of 41 cm^2 V^{-1} s^{-1}, much higher than the value of μ_{Hall}=23 cm^2 V^{-1} s^{-1}, which confirms that, at this doping level, the grain boundary scattering effect is predominant. As long as N is inferior to 10^{20} cm^{-3}, μ_{Hall} increases with the increasing carrier density. This behavior is explained by an increasing carrier concentration which facilitates the transport by creating a lower and narrower potential barrier at grain boundaries. For N superior to 1.0×10^{20} cm^{-3}, tunneling through potential barrier occurs and grain boundaries do not limit the conductivity anymore. In this case μ_{optic} and μ_{Hall} are close and decrease with the increasing carrier density, indicating that the bulk scattering becomes the main limiting factor of the electron mobility.

A high mobility value of 44.2 cm^2 V^{-1} s^{-1} was reported[17] for heavily doped sputtered ZnO:Al, in which mobility is limited by intragrain ionized impurity scattering. The relatively low mobility of LPCVD ZnO (23 cm^2 V^{-1} s^{-1} at 2.0×10^{20} cm^{-3}) indicates that additional bulk scattering phenomena occur. Ionized impurity scattering is usually considered as the limiting factor for heavily doped ZnO.[5,6,18] But, as reviewed by Ellmer,[5] several other mechanisms could explain this low mobility value, such as formation of impurity clusters, higher charge states of ionized donors (due to self-doping by oxygen vacancies), or extrinsic dopants on interstitial sites. Further investigations, such as temperature dependence of mobility measurements, are needed to gain insight into this phenomenon. Finally, our results are consistent with the temperature dependence of the resistivity of these ZnO films,[12] for which negative and positive temperature coefficients have been found near room temperature for lightly and heavily doped films, respectively. These coefficient signs are linked to transport influenced either by thermally activated potential barriers or by an intragrain scattering which increases with the temperature.

In summary, the experimental observation of a continuous transition between grain boundary scattering and intragrain scattering limited mobility is reported. This study gives a comprehensive picture of transport mechanisms in LPCVD ZnO films. It points out that, for lightly doped film (with $N<10^{20}$ cm^{-3}), the mobility can be improved by increasing the grain size. Furthermore for grain size $\delta>600$ nm, grain boundary density is too low to influence the measured mobility. For heavily doped film (with $N>10^{20}$ cm^{-3}), the mobility is limited by intragrain scattering, and improvements of the grain bulk quality are mandatory to increase the conductivity of the polycrystalline layers. A high mobility value of 36 cm^2 V^{-1} s^{-1} is measured for thick, lightly doped ($N=3.8\times10^{19}$ cm^{-3}) ZnO films having a large grain size ($\delta\sim500$ nm). This film is particularly appropriate as TCO in thin-film solar cells due to its reduced FCA, its good conductivity, and its ability to scatter light efficiently. Indeed, microcrystalline solar cells with a conversion efficiency of 10% could be fabricated on such substrate.[19]

The authors thank the Swiss Federal Government (OFEN) and the Swiss Commission for Technology and Innovation (CTI) for financial support.

[1]A. Shah, J. Meier, A. Bucechel, U. Kroll, J. Steinhauser, F. Meillaud, H. Schade, and D. Dominé, Thin Solid Films **502**, 292 (2006).
[2]J. Müller, B. Rech, J. Springer, and M. Vanecek, Sol. Energy **77**, 917 (2004).
[3]S. Faÿ, L. Feitknecht, R. Schlüchter, U. Kroll, E. Vallat-Sauvain, and A. Shah, Sol. Energy Mater. Sol. Cells **90**, 2960 (2006).
[4]J. Meier, Proceedings of the 31st IEEE Photovoltaic Specialist Conference, Lake Buena Vista, FL, 2005 (unpublished).
[5]K. Ellmer, J. Phys. D **34**, 3097 (2001).
[6]T. Minami, MRS Bull. **38**, 40 (2000).
[7]D. Mergel and Z. Qiao, J. Phys. D **35**, 794 (2002).
[8]Z. C. Jin, I. Hamberg, and C. G. Granqvist, J. Appl. Phys. **64**, 5117 (1988).
[9]N. R. Aghamalyan, E. A. Kafadaryan, R. K. Hovsepyan, and S. I. Petrosyan, Semicond. Sci. Technol. **18**, 525 (2003).
[10]I. Hamberg and C. G. Granqvist, J. Appl. Phys. **60**, R123 (1986).
[11]C. C. Marcel, N. Naghavi, G. Couturier, J. Salardenne, and J. M. Tarascon, J. Appl. Phys. **91**, 4291 (2002).
[12]J. Steinhauser, S. Faÿ, R. Schlüchter, E. Vallat, S. Y. Myong, and C. Ballif, Mater. Res. Soc. Symp. Proc. **928**, (2006).
[13]Z. Qiao, C. Agashe, and D. Mergel, Thin Solid Films **496**, 520 (2006).
[14]M. Guglielmi, E. Menegazzo, M. Paolizzi, G. Gasparro, D. Ganz, J. Pütz, M. A. Aegerter, L. Hubert-Pfalzgraf, C. Pascual, A. Duran, H. X. Willems, M. Van Bommel, L. Bèttgenbach, and L. Costa, J. Sol-Gel Sci. Technol. **13**, 679 (1998).
[15]J. Y. Seto, J. Appl. Phys. **46**, 5247 (1975).
[16]J. Bruneaux, H. Cachet, M. Froment, and A. Messad, Thin Solid Films **197**, 129 (1991).
[17]C. Agashe, O. Kluth, J. Hupkes, U. Zastrow, B. Rech, and M. Wutting, J. Appl. Phys. **95**, 1911 (2004).
[18]D. L. Young, T. J. Coutts, V. I. Kaydanov, A. S. Gilmore, and W. P. Mulligan, J. Vac. Sci. Technol. A **18**, 2978 (2000).
[19]J. Bailat, D. Dominé, R. Schlüchter, J. Steinhauser, S. Faÿ, F. Freitas, C. Bücher, L. Feitknecht, X. Niquille, T. Tscharner, A. Shah, and C. Ballif, Proceedings of the Fourth World Conference on Photovoltaic Energy Conversion, Hawaii, 2006 (unpublished), pp. 1533–1536.